

Water Soluble N-Heterocyclic Carbene-Protected Gold Nanoparticles: Size-Controlled Synthesis, Stability and Optical Properties

Kirsi Salorinne, Renee W. Y. Man, Chien-Hung Li, Masayasu Taki, Masakazu Nambo* and Cathleen M. Crudden*

Abstract: NHC-Au(I) complexes were employed in the preparation of stable, water-soluble NHC-protected gold nanoparticles. The water soluble, charged nature of the nanoparticles permitted analysis by polyacrylamide gel electrophoresis (PAGE), which showed that the nanoparticles were highly monodisperse, with tunable core diameters between 2.0 and 3.4 nm depending on the synthesis conditions. Temporal, thermal, and chemical stability of the nanoparticles were determined to be high. Treatment with thiols caused etching of the particles after 24 h, however larger plasmonic particles showed considerably greater resistance to thiol treatment. The water soluble, bio-compatible nanoparticles were shown to be promising candidates for use in photoacoustic imaging, with even the smallest nanoparticles giving a photoacoustic signal.

Gold nanoparticles represent one of the most often employed and most recognizable nanostructures.^[1] With a multitude of catalytic, imaging, drug delivery and theranostic applications, these species have attracted considerable attention. Thus unsurprisingly, recent interest in the use of *N*-heterocyclic carbenes (NHCs) as alternatives to thiols for the functionalization of gold surfaces^[2] is providing new opportunities in this important area of nanochemistry, and there are several examples of the use of these ligands to stabilize gold nanoparticles.^[3] However, if applications are to be realized in biological systems, the ability to solubilize metal nanoparticles in aqueous media is critical.

Thus far, there are very few examples of water-dispersible NHC-stabilized metal nanoparticles.^[4] In 2015, the Johnson group published a seminal paper describing Au nanoparticles stabilized with polyethylene glycol (PEG)-functionalized NHCs.^[4a] The use of the PEGylated NHC ligand provided high stability to a range of pHs and good stability under moderate, biologically relevant electrolyte concentrations. With regard to non-noble metal nanoparticles, Chaudret^[4b] described the use of sulfonate-terminated NHC ligands as stabilizing groups for Pt nanoparticles. Ravoo and Glorius have employed water-soluble NHC-stabilized metal nanoparticles in catalytic reactions, including the use of bidentate hybrid NHC-thioether ligands for the stabilization of water-soluble Pd and Au nanoparticles.^[4c-d] These systems showed good pH stability, however as they were destined for catalytic rather than biological applications, stability tests in high ionic strength media or biologically relevant nucleophiles were not reported.

Considering the potential importance of NHCs as robust and oxidatively stable ligands in nanotechnology, biosensing and drug delivery, the need to access water-soluble and biocompatible structures cannot be overstated. In this regard, we set out to prepare NHC-functionalized, water-soluble nanoparticles. Carboxylate groups were chosen due to their water solubility, pH tunability, and ease of derivatization.

We began by preparing the coordination complex NHC-Au-Cl (**1**), (Figure 1), through reaction of Me₂S-Au-Cl with the

corresponding carboxylated benzimidazolium triflate in the presence of K₂CO₃ at 60 °C.^[5] Although effective, this method was often complicated by the presence of [(NHC)₂Au]⁺OTf⁻ (**2**), sometimes in large amounts.^[6] Considering the ready availability of **2**, we also explored its use as a nanoparticle precursor despite the presence of two strong Au-NHC bonds.^[7] As shown in Figure 1, both of these starting materials gave rise to stable, water-soluble gold nanostructures.

Reduction of neutral complex **1** with NaBH₄ took place with an immediate color change to dark brown, indicating nanoparticle formation. The carboxylate functionality on the carbene ligand renders the nanoparticles water soluble when deprotonated and makes the surface of the nanoparticles charged, as required for electrophoretic mobility.^[8] Thus the purity and monodispersity of the resulting water soluble NHC-Au nanoparticles could be readily analyzed by polyacrylamide gel electrophoresis (PAGE), which is known to separate species in the gel matrix based on size.

After 5 h reaction time, nanoparticles derived from **1** gave narrow bands in the PAGE gel attributable to high monodispersity (Figure 1, lane B, **NP¹-5h**). A sample of perfectly monodisperse Au₁₀₂(pMBA)₄₄ clusters is included for comparison (lane A, pMBA = *para*-mercaptobenzoic acid).^[9]

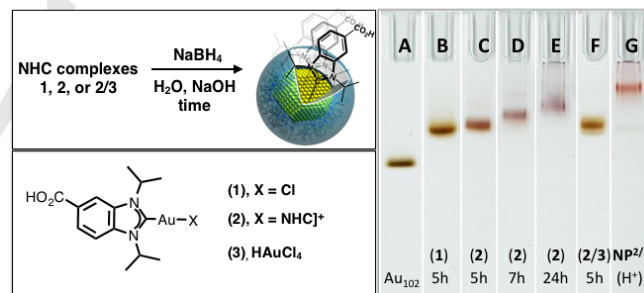


Figure 1. Synthesis of water-soluble NHC-Au nanoparticles by direct reduction of molecular NHC-Au complexes **1** or **2**, or a mixture of **2** and HAuCl₄ (**3**). PAGE (Tris-HCl/glycine) analysis of the purified products. Au₁₀₂ = Au₁₀₂(pMBA)₄₄ cluster^[9] as a reference, H⁺ = ripened NPs under acidic conditions.

The reduction of complex **2** occurred more slowly, with nanoparticles appearing only after one hour. NHC-coated nanoparticles displaying a weak surface plasmon resonance (SPR) band at 520 nm were finally isolated after 5 h (Figure 1, lane C, **NP²-5h**). Interestingly, based on their behavior on the PAGE gel, the size of the nanoparticles produced from **2** after 5 h (**NP²-5h**, lane C) was very close to those produced from complex **1** (lane B). Due to the ease of synthesis of starting complex **2**, and the similarity of the resulting particles, this method became our preferred choice.

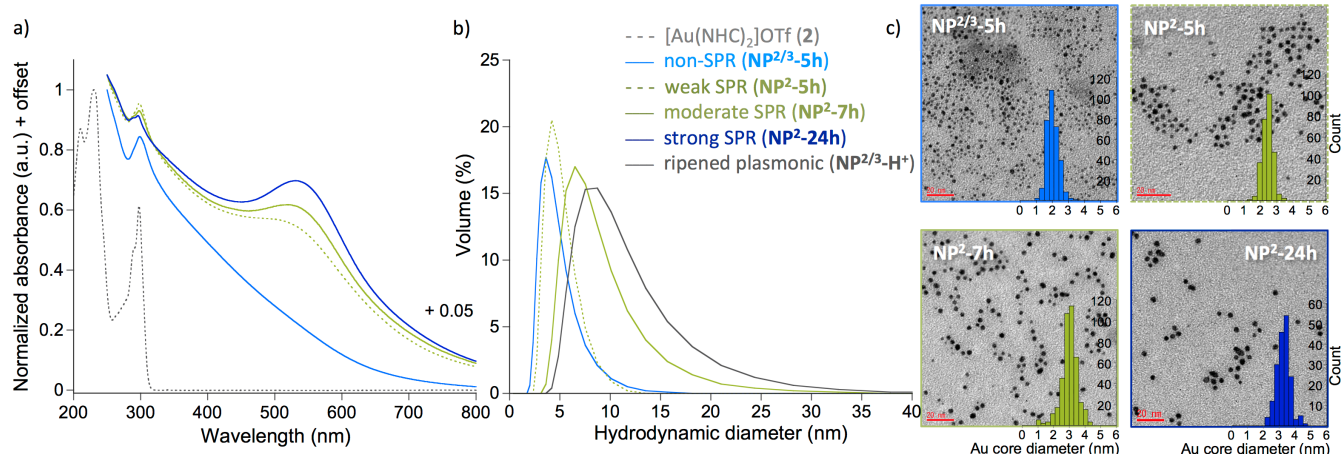


Figure 2. Representative a) UV-Vis spectra, b) DLS volume distribution and c) TEM images with size histograms of the different sized NHC-Au nanoparticles (see Table 1). UV-Vis and DLS measurements were made in basic aqueous solutions. For the larger nanoparticles (**NP²-5h**, **-7h** and **-24h**), SPR resonance is observed at 520–533 nm. The scale bar is 20 nm in all TEM images. Dotted grey = complex **2**, solid blue = non-SPR (**NP^{2/3}-5h**), dotted green = weak SPR (**NP²-5h**), solid green = moderate SPR (**NP²-7h**), solid navy = strong SPR (**NP²-24h**) and solid grey = ripened plasmonic (**NP^{2/3}-H⁺**) NHC-Au nanoparticles.

The size of the nanoparticles and the intensity of the SPR band could be controlled by varying the reaction time. Interestingly, the evolution of the NHC-Au nanoparticles to larger sizes proceeded homogeneously affording NHC-protected gold nanoparticles with narrow size distributions after 7 and 24 hrs, as evaluated by TEM and gel electrophoresis (Figure 1, lanes D and E, **NP²-7h** and **NP²-24h**, see also Supporting Information). The bands displayed various colors indicative of the particles being at the edge of the plasmonic regime (ca. 2nm).^[10]

Since only surface Au atoms are ligated by NHCs, we also examined the effect of added HAuCl₄ (**3**) as a source of unligated gold (see Supporting Information for experimental details). Using **2** and **3** as starting materials, nanoparticles formed much more quickly, with reaction mixtures becoming dark brown immediately. The resulting nanoclusters were similar in size to **NP¹-5h** as determined by PAGE and TEM (Figure 1, lanes B and F). Importantly, TGA and XPS analyses indicated that both methods lead to nanoparticles with the same NHC: Au ratio within experimental error (Figure S9), and thus only data for **NP^{2/3}-5h** are shown below (see Supporting Information for **NP¹-5h**).

UV-Vis analysis confirmed the presence of plasmonic transitions of varying strength for the different nanoparticles (Figure 2, Table 1). TEM analysis confirmed that nanoparticle cores ranged in size from 2.4 (± 0.3) nm for NHC-Au nanoparticles exhibiting a weak SPR band (**NP²-5h**) to 3.3 (± 0.4) nm for nanoparticles with a strong SPR band (**NP²-24h**). Nanoparticles with a moderate SPR band (**NP²-7h**) had core sizes of 3.0 (± 0.5) nm. NHC-Au nanoparticles (**NP¹-5h** and **NP^{2/3}-5h**) obtained from reductions of both complexes **1** and **2/3** exhibited featureless UV-Vis spectra devoid of an SPR band. These were estimated by TEM to have an average size of 2.0 (± 0.4) nm.

Evidence of NHC binding on Au nanoparticle surface was afforded by XPS studies, which showed the carbene N 1s peak at ~401 eV (Figure S10), consistent with our previous studies.^[2b] In addition, we observed the binding energy of the alkyl/aromatic carbon at ~285 eV, carboxylate carbon at ~290 eV, and also π to π* at ~291.5 eV from the C 1s spectrum (Supporting Information, Figure S11).^[11]

Table 1. Structural properties of NHC-Au nanoparticles (NP).

NP	Core _{TEM} (nm) ^[a]	Au:NHC (%) ^[b]	Au:NHC _{calc} (%) ^[c]	NP _{DLS} (nm) ^[d]	NP _{calc} (nm) ^[c]	SPR (nm) ^[e]
NP^{2/3}-5h	2.0 ± 0.4	85.0 : 15.0	79.9 : 20.1	4.4 ± 1.7	3.8	–
NP²-5h	2.4 ± 0.3	n.d.	n.d.	4.8 ± 1.5	4.3	520
NP²-7h	3.0 ± 0.5	90.1 : 9.9	90.5 : 9.5	8.1 ± 3.0	4.8	525
NP²-24h	3.3 ± 0.4	n.d.	n.d.	n.d.	n.d.	533
NP^{2/3}-H⁺	4.7 ± 0.8	n.d.	n.d.	10.2 ± 4.6	6.1	520

n.d. = not determined. [a] Average diameter of the gold core as determined by TEM. [b] NP metal and ligand content as determined by TGA analysis. [c] Calculated values for metal-to-ligand ratio and hydrodynamic diameter were based on TEM core size and surface coverage of NHC ligand^[2b] according to the method described by Murray^[12] (see Supporting Information for details). [d] Average hydrodynamic diameter of NHC-Au NPs in H₂O as determined by DLS and reported as volume distribution. [e] Location of surface plasmon resonance band in H₂O as determined by UV-Vis spectroscopy.

Information about the extent of surface functionalization was obtained by TGA analysis. For the larger NHC-Au nanoparticles (**NP²-7h**) with a moderate SPR band, the Au:NHC ratio was determined to be 90:10, whereas smaller nanoparticles (**NP¹-5h** and **NP^{2/3}-5h**) had a ratio of 85:15, both of which correlated well with the respective core sizes based on TEM (Table 1 and S9). Remarkably, nanoparticles prepared either from neutral complex **1** or a mixture of **2/3**, show almost identical TGA curves, both displaying the same NHC to gold ratio (Figure S9).

Dynamic light scattering (DLS) studies provided the hydrodynamic size of the nanoparticles including both the gold core and the protecting NHC ligand layer, which affords more accurate assessment of the predominant size of the nanoparticles in solution (Table 1).^[13] The hydrodynamic diameters obtained by DLS in basic aqueous solution were slightly larger than those determined by TEM, but were within error considering the higher standard deviation of the DLS method, particularly with nanoparticles smaller than 5 nm (Figure 2b).^[14]

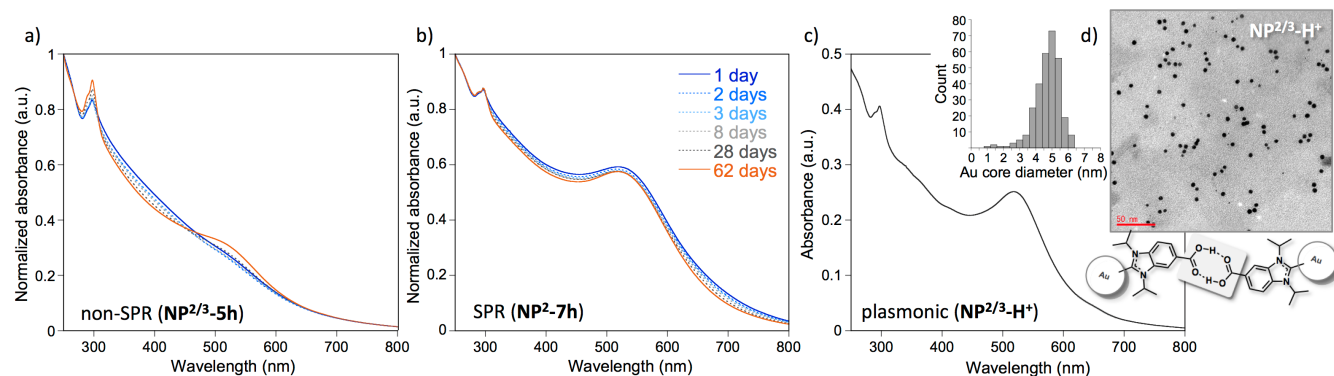


Figure 3. a-b) Long-term stability of NHC-Au nanoparticles in aqueous solution (pH 8) showing UV-Vis spectra of non-SPR ($\text{NP}^{2/3}\text{-5h}$) and SPR ($\text{NP}^2\text{-7h}$) nanoparticles during 62 days. c-d) Instability of the protonated nanoparticles in organic solvents leads to plasmonic particles ($\text{NP}^{2/3}\text{-H}^+$): UV-Vis spectrum in aqueous solution (basic pH) showing an SPR band at 520 nm and TEM image with a size histogram displaying an average size of 4.7 ± 0.8 nm. Scale bar is 50 nm.

Having established a robust synthetic route to water-soluble NHC nanoparticles of varying sizes, we then examined the stability of the NHC-Au nanoparticles in aqueous solution under different conditions. Long-term stability was tested in basic aqueous solutions (pH 8 and pH 10) and monitored by UV-Vis spectroscopy. The smaller non-SPR nanoparticles ($\text{NP}^{2/3}\text{-5h}$) were stable up to one month under these conditions, after which time a small SPR band at ca. 520 nm started to appear (Figure 3a). Larger SPR nanoparticles ($\text{NP}^2\text{-7h}$) were stable for at least two months with only small changes in their UV-Vis spectra over that time (Figure 3b). No difference in the stability of the nanoparticles was observed between pH 8 and 10. Adjusting the pH of the solution to acidic (pH 2), however, resulted in precipitation of a black solid, which could be redissolved in basic media (pH 10). This pH cycle could be repeated at least five times without any significant changes in the UV-Vis spectra of the non-SPR nanoparticles ($\text{NP}^{2/3}\text{-5h}$). For the larger nanoparticles ($\text{NP}^2\text{-7h}$), a small sharpening and slight blue shifting of the SPR band from 520 to 508 nm was observed (Figure S13).^[15]

In protonated form, the NHC-Au nanoparticles are soluble in organic solvents, but have a much shortened lifespan. Within 1–2 days, particles were observed to aggregate and form insoluble solids (MeOH/EtOH/iPrOH) that could not be redissolved. In CH_3CN or DMF, on the other hand, ripening to larger stable plasmonic particles took place (4.7 ± 0.8 nm, $\text{NP}^{2/3}\text{-H}^+$), which could be redissolved in water at basic pH and isolated by centrifugal ultrafiltration (Figure 1, lane G and Figure 3c-d). This is most likely due to hydrogen bonding interactions between the protonated carboxylic acid groups of the neighboring nanoparticles that bring the nanoparticles closer together and facilitate the aggregation^[4c] or ripening processes.

The stability of the NHC-Au nanoparticles in the presence of electrolytes¹⁶ and glutathione was also examined. A 150 mM NaCl solution was chosen to simulate physiologically relevant saline concentrations and the stability of the nanoparticles was monitored both by UV-Vis and DLS experiments. The non-SPR nanoparticles ($\text{NP}^{2/3}\text{-5h}$) were stable for at least for 3 days in the electrolyte solution, with a small SPR band starting to emerge at 510 nm after 7 days (Figure 4a). Larger nanoparticles ($\text{NP}^2\text{-5h}$) showed very high stability, with small sharpening of the SPR band visible after 7 days, suggesting a modest ripening of the particles (Figure 4b). TEM analysis showed that after 7 days

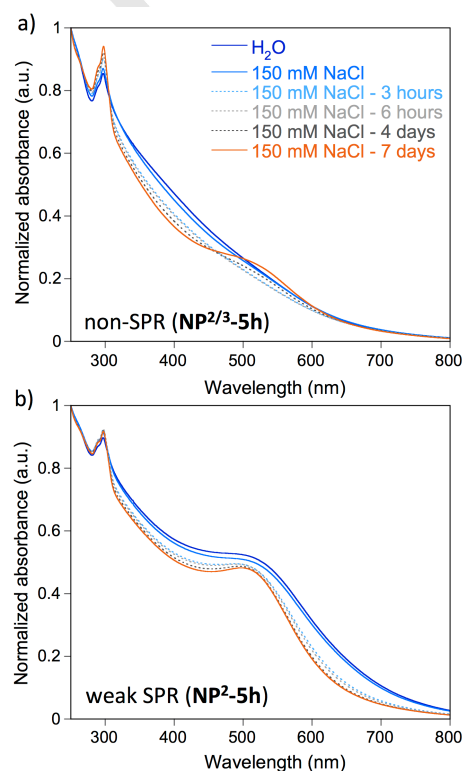


Figure 4. UV-Vis spectra of a) non-SPR ($\text{NP}^{2/3}\text{-5h}$) and b) weak SPR ($\text{NP}^2\text{-5h}$) NHC-Au nanoparticles in aqueous 150 mM NaCl solution at pH 8 during 7 days time.

both types of nanoparticles became slightly less monodisperse with the formation of some larger particles in both cases, accounting for approximately 10% of the particles observed, $\pm 2\%$ (Figure S15).

In biological media, glutathione (GSH) is typically found in 0.5 – 10 mM concentrations,^[17] therefore, NHC-Au nanoparticles (31 $\mu\text{g}/\text{mL}$) were exposed to 2 mM GSH solution under slightly basic conditions (pH 8). This corresponds to a large excess of GSH relative to the nanoparticle concentration.^[18] Under these conditions, non-SPR ($\text{NP}^{2/3}\text{-5h}$) nanoparticles showed low stability and considerable decomposition of the particles to molecular

NHC-Au species within 24 hrs (Figure S16). Larger SPR nanoparticles (**NP^{2-5h}**) were more resistant to GSH treatment such that a reasonable signal at 515 nm was still present after 24 hrs. At higher NHC-Au nanoparticle concentrations (2.2 mg/mL), under the same conditions, both TEM and PAGE analyses showed etching of the particles, however the larger SPR (**NP^{2-5h}**) particles still displayed an SPR band even after 5 hrs GSH treatment (Figure S17 and S18).

These results are related to the PEG-functionalized NHC protected Au nanoparticles reported by the Johnson group,^[4a] which showed long-term stability in aqueous solution, but were susceptible to etching or aggregation under high electrolyte concentrations or during long exposure to various thiols.^[4a] Thus, the strong NHC-Au bond does appear to be highly effective at preventing nanoparticle decomposition over time, but the lower surface density of NHCs compared to thiols on gold may provide space for thiol attack at accessible surface gold atoms.

Finally, we probed the possibility of employing these water-soluble nanoparticles in photoacoustic (PA) imaging, which has attracted much attention as a bio-imaging technique with deep tissue penetration and good spatial resolution.^[19] Irradiating an aqueous solution of nanoparticles with a pulsed laser beam (532 nm) resulted in a reproducible acoustic wave signal (Figure 5). Remarkably, even the smallest nanoparticles (**NP^{2-5h}**, 2.4 nm), that exhibited only a weak SPR band at 520 nm, gave a detectable PA signal as shown in Figure 5. The intensity of the PA signal correlated linearly with the concentration of nanoparticles, showing that the nanoparticles are potentially interesting photoacoustic probes.

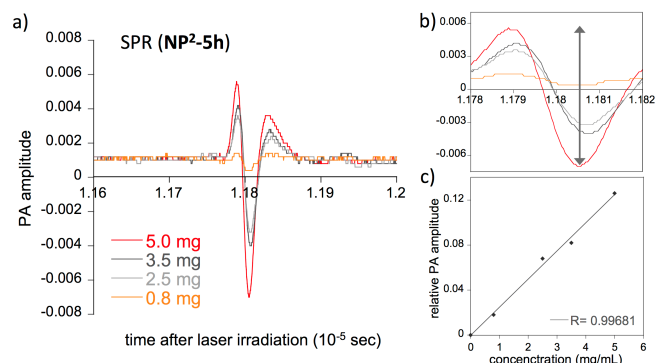


Figure 5. a) Acoustic wave signal detected after irradiating an aqueous solution of weak SPR nanoparticles (**NP^{2-5h}**) at 532 nm using a pulsed laser beam. b) Zoom-in of the PA signal showing the signal intensity (grey arrow, shown for the most intense signal) used for the calculation of the relative PA amplitude as a function of sample concentration shown in c).

In conclusion, we have described a bottom-up approach for the synthesis of novel NHC-protected gold nanoparticles employing water soluble, pH-tunable NHCs. The use of bis NHC or mono NHC Au complexes as starting materials provided highly monodisperse NHC-protected nanoparticles. Size evolution of the nanoparticles occurred with time, but remarkably, larger particles were also formed with a high degree of monodispersity. The use of HAuCl₄ as an additive to promote nanoparticle formation was accomplished without any effect on the density of NHC ligands on the surface. High temporal stability was observed and reasonable stability to ionic strengths of biological

relevance. Instability to thiols continues to be a challenge with these otherwise highly effective ligands, however larger nanoparticles showed resistance to degradation over reasonable time frames for biological applications. The potential for the use of these nanoparticles in photoacoustic imaging was also demonstrated. Further development of stable NHC-protected nanoparticles and their applications in bio-imaging are currently being examined in our laboratory.

Acknowledgements

This work was supported by a KAKENHI grant from the JSPS (26288023 to C.M.C.). JSPS and NU are acknowledged for funding of this research through The World Premier International Research Center Initiative (WPI) program. We thank Dr. Tanja Lahtinen from the University of Jyväskylä for providing Au₁₀₂(pMBA)₄₄ as a reference sample. Mr. Takaji Nemoto and Mr. Yuichiro Uehata (CORNES Technologies Ltd.) are thanked for assistance with measurement of photoacoustic signal. Profs. Kenichiro Itami, Shigehiro Yamaguchi and Tetsuya Higashiyama are thanked for generous access to their facilities at ITbM/NU. QU and the Canada Foundation for Innovation are thanked for infrastructure that was used in support of this project. The Natural Sciences and Engineering Research Council of Canada (NSERC) is thanked for support of CHL.

Conflict of interests

The authors declare no conflict of interest.

Keywords: N-heterocyclic carbenes • gold nanoparticle • water-soluble • stability • photoacoustic

- [1] a) R. Jin, C. Zeng, M. Zhou, Y. Chen, *Chem. Rev.* **2016**, *116*, 10346–10413; b) E.-K. Lim, T. Kim, S. Paik, S. Haam, Y.-M. Huh, K. Lee, *Chem. Rev.* **2015**, *115*, 327–394; c) S. Eustis, M. A. El-Sayed, *Chem. Soc. Rev.* **2006**, *35*, 209–217; d) M. N. Hopkinson, C. Richter, M. Schedler, F. Glorius, *Nature* **2014**, *510*, 485–496; e) C. Gautier, T. Bgrgi, *ChemPhysChem* **2009**, *10*, 483–492; f) S. Knoppe, T. Bgrgi, *Acc. Chem. Res.* **2014**, *47*, 1318–1326.
- [2] a) A. V. Zhukhovitskiy, M. J. MacLeod, J. A. Johnson, *Chem. Rev.* **2015**, *115*, 11503; b) C. M. Crudden, J. H. Horton, I. I. Ebralidze, O. V. Zenkina, A. B. McLean, B. Drevniok, Z. She, H. B. Kraatz, N. J. Mosey, T. Seki, E. C. Keske, J. D. Leake, A. Rousina-Webb, G. Wu, *Nature Chem.* **2014**, *6*, 409; c) A. V. Zhukhovitskiy, M. G. Mavros, T. Van Voorhis, J. A. Johnson, *J. Am. Chem. Soc.* **2013**, *135*, 7418; d) C. M. Crudden, J. H. Horton, M. R. Narouz, Z. Li, C. A. Smith, K. Munro, C. J. Baddeley, C. R. Larrea, B. Drevniok, B. Thanabalasingam, A. B. McLean, O. V. Zenkina, I. I. Ebralidze, Z. She, H. B. Kraatz, N. J. Mosey, L. N. Saundes, A. Yagi, *Nature Commun.* **2016**, *7*, 12654; e) T. Weidner, J. E. Baio, A. Mundstock, C. Grosse, S. Karthäuser, C. Bruhn, U. Siemeling, *Aust. J. Chem.* **2011**, *64*, 1177; f) G. Wang, *et al.*, *Nat. Chem.* **2017**, *9*, 152–156.
- [3] a) M. J. MacLeod, J. A. Johnson, *J. Am. Chem. Soc.* **2015**, *137*, 7974; b) E. A. Baquero, S. Tricard, J. C. Flores, E. de Jesús, B. Chaudret, *Angew. Chem. Int. Ed.* **2014**, *53*, 13220; c) A. Ferry, K. Schaepe, P. Tegeder, C. Richter, K. M. Chepiga, B. J. Ravoo, F. Glorius, *ACS Catal.* **2015**, *5*, 5414; d) A. Rühling, K. Schaepe, L. Rakers, B. Vonhören, P. Tegeder, B. J. Ravoo, F. Glorius, *Angew. Chem. Int. Ed.* **2016**, *55*, 5856.

- [4] a) M. J. MacLeod, J. A. Johnson, *J. Am. Chem. Soc.* **2015**, *137*, 7974; b) E. A. Baquero, S. Tricard, J. C. Flores, E. de Jesús, B. Chaudret, *Angew. Chem. Int. Ed.* **2014**, *53*, 13220; *Angew. Chem.* **2014**, *126*, 13436; c) A. Ferry, K. Schaepe, P. Tegeder, C. Richter, K. M. Chepiga, B. J. Ravoo, F. Glorius, *ACS Catal.* **2015**, *5*, 5414; d) A. Rühling, K. Schaepe, L. Rakers, B. Vonhören, P. Tegeder, B. J. Ravoo, F. Glorius, *Angew. Chem. Int. Ed.* **2016**, *55*, 5856; *Angew. Chem.* **2016**, *128*, 5950.
- [5] A. Collado, A. Gómez-Suárez, A. R. Martin, A. M. Z. Slawin, S. P. Nolan, *Chem. Commun.* **2013**, *49*, 5541.
- [6] Reaction of NHC halide salts under these conditions produce NHC-AuX complexes in high yields, whereas [(NHC)₂Au]⁺ species are obtained as major product when NHC salts with non-coordinating anions, such as OTf⁻, are used. See for example, a) R. Jothibasu, H. V. Huynh, L. L. Koh, *J. Organomet. Chem.* **2008**, *693*, 374; b) H. M. J. Wang, C. Y. L. Chen, I. J. B. Lin, *Organometallics*, **1999**, *18*, 1216.
- [7] Despite the strength of the metal-carbon bond in NHC metal complexes, there are many examples where the cleavage of the metal carbon bond does take place. See for example: a) C. M. Crudden, D. P. Allen, *Coord. Chem. Rev.* **2004**, *248*, 2247; b) D. S. McGuinness, M. J. Green, K. J. Cavell, B. W. Skelton, A. H. White, *J. Organomet. Chem.* **1998**, *565*, 165; c) D. P. Allen, C. M. Crudden, L. A. Calhoun, R. Wang, *J. Organomet. Chem.* **2004**, *689*, 3203.
- [8] a) K. Kimura, N. Sugimoto, S. Sato, H. Yao, Y. Negishi, T. Tsukuda, *J. Phys. Chem. C* **2009**, *113*, 14076. b) N. Surugau, P. L. Urban, *J. Sep. Sci.* **2009**, *32*, 1889.
- [9] Structurally known Au₁₀₂(pMBA)₄₄ cluster was used as a reference compound due to similar carboxylic acid decorated surface, a) P. D. Jadzinsky, G. Calero, C. J. Ackerson, D. A. Bushnell, R. G. Kornberg, *Science* **2007**, *318*, 430; b) Y. Levi-Kalishman, P. D. Jadzinsky, N. Kalishman, H. Tsunoyama, T. Tsukuda, D. A. Bushnell, R. D. Kornberg, *J. Am. Chem. Soc.* **2011**, *133*, 2976.
- [10] a) S. Malola, L. Lehtovaara, J. Enkovaara, H. Häkkinen, *ACS Nano* **2013**, *7*, 10263; b) K. Iida, M. Noda, K. Ishimura, K. Nobusada, *J. Phys. Chem. A* **2014**, *118*, 11317.
- [11] a) J. W. Park, J. S. Shumaker-Parry, *ACS Nano*, **2015**, *9*, 1665; b) H. J. Lee, A. C. Jamison, Y. Yuan, C. H. Li, S. Rittikulsittichai, I. Rusakova, T. R. Lee, *Langmuir* **2013**, *29*, 10432; c) M. M. Browne, G. V. Lubarsky, M. R. Davidson, R. H. Bradley, *Surf. Sci.* **2004**, *553*, 155.
- [12] a) M. J. Hostettler, J. E. Wingate, C. J. Zhong, J. E. Harris, R. W. Vachet, M. R. Clark, J. D. Londono, S. J. Green, J. J. Stokes, G. D. Wignall, G. L. Glish, M. D. Porter, N. D. Evans, R. W. Murray, *Langmuir* **1998**, *14*, 17; b) W. P. Wuelfing, S. M. Gross, D. T. Miles, R. W. Murray, *J. Am. Chem. Soc.* **1998**, *120*, 12696.
- [13] Since our NHC-stabilized Au nanoparticles are water soluble only when deprotonated, an additional layer of hydrated sodium cations needs to be accounted for when calculating the hydrodynamic size of the nanoparticles. K. Salorinne, T. Lahtinen, S. Malola, J. Koivisto, H. Häkkinen, *Nanoscale* **2014**, *6*, 7823.
- [14] B. N. Khlebtsov, N. G. Khlebtsov, *Coll. J.* **2011**, *73*, 118.
- [15] After each step of the repeated pH cycle, which entails precipitation and redissolution of the particles, the product is collected by centrifugation. This additionally removes small impurities and insoluble particles that may be present in the original solution, which can also account for the observed blue shift seen during the cycle.
- [16] a) T. Laaksonen, P. Ahonen, C. Johans, K. Kontturi, *Chem. Phys. Chem.* **2006**, *7*, 2143; b) R. Pamies, J. H. Cifre, V. F. Espin, M. Collado-Gonzalez, F. G. D. Baños, J. G. de la Torre, *J. Nanopart. Res.* **2014**, *16*, 2376.
- [17] a) G. K. Balendiran, R. Dabur, D. Fraser, *Cell Biochem. Funct.* **2004**, *22*, 343; b) P. Maher, *Ageing Res. Rev.* **2005**, *4*, 288.
- [18] Based on TGA data, 1 mg/mL of NHC-Au nanoparticles contain 1.4 mM (non-SPR, NP²³-5h) and 0.8 mM (weak SPR, NP²-5h) concentration of NHC ligands in comparison to 2 mM of GSH.
- [19] a) A. de la Zerda, J.-W. Kim, E. I. Galanzha, S. S. Gambhir, V. P. Zharov, *Contrast Media Mol. Imaging*, **2011**, *6*, 346. b) J. Yao, L. Wang, *Photoacoustics* **2014**, *2*, 87. c) K. Pu, A. J. Shuhendler, J. V. Jokerst, J. Mei, S. G. Gambhir, Z. Bao, J. Rao, *Nature Nanotech.* **2014**, *9*, 233. d) L. Nie, X. Chen, *Chem. Soc. Rev.* **2014**, *43*, 7132; e) Y. Liu, J. He, K. Yang, C. Yi, Y. Liu, L. Nie, N. M. Khashab, X. Chen, Z. Nie, *Angew. Chem. Int. Ed.* **2015**, *54*, 15809; *Angew. Chem.* **2015**, *127*, 16035.